Electron Attachment to Dye-Sensitized Solar Cell Components: Rhodanine and Rhodanine-3-acetic Acid

ARTICLE *in* THE JOURNAL OF PHYSICAL CHEMISTRY C · DECEMBER 2009

Impact Factor: 4.77 · DOI: 10.1021/jp910595v

3 AUTHORS, INCLUDING:

Derek Jones
Italian National Research Council
103 PUBLICATIONS **1,466** CITATIONS
SEE PROFILE

Stanislav A Pshenichnyuk
Institute of Physics of Molecules and Crystals
58 PUBLICATIONS **293** CITATIONS
SEE PROFILE

Electron Attachment to Dye-Sensitized Solar Cell Components: Rhodanine and Rhodanine-3-acetic Acid

Alberto Modelli,*,† Derek Jones,‡ and Stanislav A. Pshenichnyuk§

Università di Bologna, Dipartimento di Chimica "G. Ciamician", via Selmi 2, 40126 Bologna, Italy, Centro Interdipartimentale di Ricerca in Scienze Ambientali, via S. Alberto 163, 48123 Ravenna, Italy, ISOF, Istituto per la Sintesi Organica e la Fotoreattività, C.N.R., via Gobetti 101, 40129 Bologna, Italy, and Institute of Physics of Molecules and Crystals, Ufa Research Center of RAS, October Prospect, 151, Ufa 450075, Russia

Received: November 6, 2009; Revised Manuscript Received: December 11, 2009

The energies of electron attachment associated with temporary occupation of π^* and σ^* virtual orbitals of the pentaheterocyclic rhodanine molecule are measured in the gas phase with electron transmission spectroscopy. The corresponding orbital energies of the neutral molecule, supplied by B3LYP/6-31G(d) calculations and scaled using an empirically calibrated linear equation, are compared with the experimental vertical attachment energies. The same computational procedure is applied to rhodanine-3-acetic acid, proposed as a possible component of dye-sensitized solar cells. In addition, the (positive) vertical and adiabatic electron affinities are evaluated at the B3LYP/6-31+G(d) level. The calculations also indicate a thermodynamic tendency toward dissociation of the ring H_2C-S bond of the molecular anion. Dissociative electron attachment spectroscopy is used to measure the total anion current, as a function of the incident electron energy, and detect with a mass filter the negative fragments generated through the dissociative decay channels of the molecular anion in the 0−4 eV energy range. In rhodanine, only two intense negative fragments are observed due to loss of a hydrogen atom or a neutral ketene ($H_2C=C=O$) molecule from the molecular anion. In the $-CH_2COOH$ derivative, in addition to these two dissociative channels, a great number of negative fragments are observed, mainly at zero electron energy, which often imply the occurrence of multiple bond cleavage and complex atomic rearrangements. These results cast serious doubts upon the stability of dyes containing rhodanine-3-acetic acid under conditions of excess negative charge.

Introduction

The most abundant source of energy on earth is solar energy. The solar energy reaching the earth in 1 h is equal to the current global annual energy consumption. The conversion of that energy into electrical energy is, therefore, seen as one of the most promising solutions for the substitution of fossil fuels. Although inorganic semiconductors, and especially silicon in various forms,[1] are being increasingly employed in photovoltaic conversion, organic alternatives may show advantages in terms of cost and flexibility in their manufacture and employment.[2] Within this context, alternative cheaper photovoltaic devices, such as dye-sensitized solar cells, have received considerable attention over the past decade.[2−7] Optimization of the performance of a solar cell involves many parameters.[5] However, a key step in the complex sequence of processes that lead to the generation of an electric current is absorption of light by the dye anchored on a TiO_2 surface with electron injection from the excited dye into the conduction band of TiO_2. Clearly, long-term stability of the whole system is also an important requirement.

Two main categories of dyes have been investigated as sensitizers, metal−organic complexes and metal-free organic dyes.[5,6] The latter generally consist of conjugated oligomers with reduced band gaps[5] or large π systems combining donor and acceptor blocks.[7−10] Recently, encouraging results (energy conversion efficiency of 5.8%) were obtained[9] using a dye where a triphenylamine derivative (donor block) is connected through two ethene double bonds to rhodanine-3-acetic acid (**Rd-aa**; see Chart 1). Light absorption causes an intramolecular charge transfer from the donor group to the rhodanine ring acceptor, anchored to TiO_2 via the carboxyl group.

CHART 1

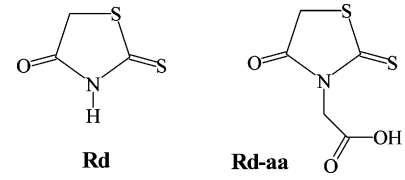

Rd **Rd-aa**

Compounds based on the five-membered heterocyclic ring of rhodanine (**Rd**) have also been found to possess important biochemical and therapeutic properties, acting as novel and selective inhibitors against dual-specificity phosphatases[11] as well as exhibiting antidiabetic,[12] antifungal,[13] antimicrobial,[14] and hypoglycemic[15] activity. In addition, rhodanine derivatives are important reagents in coordination chemistry and form coordination complexes with various metal ions.[16]

Because of their numerous applications, the chemical properties of **Rd** derivatives have received a great deal of attention. However, except for a photoelectron spectroscopy study of the outermost filled molecular orbitals (MOs) of **Rd**,[17] little is known of their electronic structures. In particular, to our

* To whom correspondence should be addressed. Tel: +39 051 2099522. Fax: +39 051 2099456. E-mail: alberto.modelli@unibo.it (A.M.), d.jones@isof.cnr.it (D.J.), sapsh@anrb.ru (S.A.P.).

† Università di Bologna and Centro Interdipartimentale di Ricerca in Scienze Ambientali.

‡ Istituto per la Sintesi Organica e la Fotoreattività, C.N.R.

§ Ufa Research Center of RAS.

10.1021/jp910595v
Published on Web 12/28/2009

knowledge, data on their empty level structures (related to the electron-acceptor properties required in the above-mentioned dyes) have not appeared in the literature.

The electron transmission spectroscopy (ETS) technique devised by Sanche and Schulz[18] is still one of the most suitable means for observing the formation of temporary anions in the gas phase and measuring negative electron affinities (EAs). The ETS technique takes advantage of the sharp variations in the total electron−molecule scattering cross section caused by resonance processes, namely, temporary capture of electrons with appropriate energy and angular momentum into empty MOs.[19] Electron attachment is rapid with respect to nuclear motion so that temporary anions are formed in the equilibrium geometry of the neutral molecule. The measured vertical attachment energies (VAEs) are the negative of the vertical EAs.

Additional information on the fate of the temporary molecular anions observed in ETS can be supplied by dissociative electron attachment spectroscopy (DEAS),[19,20] which measures the yield of mass-selected negative ions as a function of impact electron energy. Under suitable energetic conditions, the decay of unstable molecular anions formed by resonance attachment can follow a dissociative channel that generates negative and neutral fragments, in kinetic competition with simple re-emission of the extra electron. The DEAS technique can thus reveal the occurrence of dissociative processes upon anion formation. In connection with the use of **Rd-3aa** in dyes for solar cells, the rhodanine ring is a good electron acceptor due to the large EA of the π (C═S) functional group[21,22] and also contains σ (S−C) bonds. Previous DEA studies[23,24] of thioalkyl derivatives have shown that S−C bonds are prone to cleavage upon electron addition. The occurrence of ring opening under conditions of excess negative charge would, of course, damage the dye and reduce the long-term stability of the whole device.

In the present study, the empty-level structures of unsubstituted **Rd** and its 3-acetic acid derivative **Rd-aa** are analyzed by means of the above-mentioned spectroscopic techniques and suitable theoretical calculations. The density functional theory (DFT) method is employed to reproduce the energies of vertical electron attachment and characterize the nature of the corresponding temporary anion states. DFT calculations are also used to evaluate the stability of the ground anion state (i.e., positive EA) and the thermodynamic energy thresholds for production of the fragment anions detected in the DEA spectra.

Experimental Methods

Our electron transmission apparatus is in the format devised by Sanche and Schulz[18] and has been previously described.[25] To enhance the visibility of the sharp resonance structures, the impact energy of the electron beam is modulated with a small ac voltage, and the derivative of the electron current transmitted through the gas sample is measured directly by a synchronous lock-in amplifier. Each resonance is characterized by a minimum and a maximum in the derivative signal. The energy of the midpoint between these features is assigned as the VAE. The spectrum of rhodanine was obtained using the apparatus in the "high-rejection" mode[26] and is, therefore, related to the nearly total scattering cross section. The electron beam resolution was about 50 meV (fwhm). The energy scale was calibrated with reference to the $(1s^1 2s^2)^2S$ anion state of He. The estimated accuracy is ±0.05 or ±0.1 eV, depending on the number of decimal digits reported. The rhodanine sample (commercially available) was heated to about 75 °C to obtain a suitable vapor pressure.

The collision chamber of the ETS apparatus has been modified[27] to allow for ion extraction at 90° with respect to the incident electron beam direction. Ions are then accelerated and focused toward the entrance of a quadrupole mass filter. Alternatively, the total anion current can be collected and measured with a picoammeter at the walls of the collision chamber (about 0.8 cm from the electron beam). Measurements of the total and mass-selected anion currents were obtained with an incident electron beam current about twice as large as that used for the ET experiment. The energy spread of the electron beam increased to about 110 meV, as evaluated from the width of the SF_6^- signal at zero energy used for calibration of the energy scales.

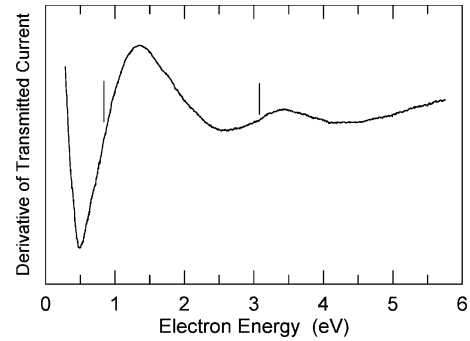

Figure 1. Derivative of transmitted current, as a function of electron energy, in gas-phase rhodanine. Vertical lines locate the VAEs.

Calculations were performed with the Gaussian 03 set of programs.[28] Evaluation of the virtual orbital energies (VOEs) of the neutral molecule was performed at the B3LYP/6-31G(d) level.[29] The vertical electron affinity (EA_v) was calculated as the difference between the total energy (only electronic contributions) of the neutral and the lowest anion state, both in the optimized geometry of the neutral state, using the B3LYP hybrid functional with the standard 6-31+G(d) basis set. The adiabatic electron affinity (EA_a) was obtained as the energy difference between the neutral and the lowest anion state, each in its optimized geometry.

Results and Discussion

Empty Level Structure: ET Spectrum of Rd and Calculated VAEs and EAs. Rd possesses two empty antibonding π^* MOs mainly localized on the nonadjacent C═S and C═O double bonds. Electron addition to the former is expected to give rise to a stable (thus, not observable with ETS) anion state, as in the case of di-*tert*-butylthioketone,[21,22] whereas electron capture into the π^*_{CO} MO should occur around 1 eV (π^*_{CO} VAE = 1.15 eV in cyclopentanone[22]). In addition, because of the presence of third-row elements (sulfur atoms), low-energy empty σ^* MOs are also to be expected.[22]

The ET spectrum of **Rd** in the 0−6 eV energy range is reported in Figure 1. Two distinct resonances are displayed, centered at 0.84 and 3.1 eV, in agreement with the above qualitative prediction of a stable (or very close to zero energy) π^*_{CS} anion state and a π^*_{CO} anion state around 1 eV. For a more accurate interpretation of the spectral features, theoretical calculations were carried out.

An adequate approach for describing unstable anion states involves difficulties not encountered for neutral or cation states.[30−33] The most correct method is, in principle, the calculation of the total scattering cross section with the use of continuum functions, but complications arise from the lack of an accurate description of the electron−molecule interaction.[34]

However, it has been demonstrated[30,32] that good linear correlations can be obtained between the $\pi^*_{C=C}$ VAEs measured

TABLE 1: B3LYP/6-31G(d) VOEs (eV) and Scaled VOEs (See Text) of Rd and Rd-aa and Measured VAEs of Rd

	orbital	VOE	scaled VOE	VAE
Rd	σ^*_{CS}	1.037	2.54	3.1
	π^*_{CO}	−0.088	1.14	
	σ^*_{CS}	−0.335	0.80	0.84
	π^*_{CS}	−2.085	−0.47	
Rd-aa	σ^*_{CS}	1.207	2.76	
(conformer **1**)	π^*_{COOH}	−0.137	1.10	
	π^*_{CO}	−0.170	1.07	
	σ^*_{CS}	−0.204	0.97	
	π^*_{CS}	−2.005	−0.40	

in unsaturated hydrocarbons and the corresponding virtual orbital energies (VOEs) of the neutral molecules obtained with simple Hartree−Fock calculations, using basis sets that do not include diffuse functions. More recently, it has been shown[35] that the neutral-state π^* VOEs obtained with DFT B3LYP/6-31G(d) calculations also supply a good linear correlation with the corresponding VAEs measured over a variety of different families of unsaturated compounds, including heterosubstituted hydrocarbons. A more accurate correlation is expected if the scaling equation is calibrated with "training" compounds structurally close to the subject molecule. For this reason, the use of the B3LYP scaling[35] (VAE = 0.805434 × VOE + 1.21099) to predict the π^* VAEs of **Rd** and **Rd-aa** seems to be more appropriate. The scaling procedure can be applied as well to σ^* VOEs, but it has been shown[36] that great caution is needed when the molecular structures or the nature of the σ^* MOs are different from those of the family of compounds used for calibration of the linear equation employed. A correlation calibrated with σ^*_{CS} VAEs has not been reported; thus, we tentatively use a correlation found (VAE = 1.2658 × VOE + 1.2278)[37] with σ^* (C−Br) VAEs and the corresponding B3LYP/6-31G(d) VOEs of bromoalkanes.

The B3LYP/6-31G(d) energies of the first four empty MOs of **Rd** are given in Table 1. Figure 2 is a representation of their localization properties. As expected, the lowest unoccupied MO (LUMO) possesses mainly π^*_{CS} character. Less expectedly, according to the calculations, the second empty MO is a ring S−C antibonding orbital of σ^* symmetry, lying at slightly lower energy than that of the mainly π^*_{CO} MO. The fourth empty MO, at higher energy, is again a ring σ^* MO with S−C antibonding character. Quite similar energy sequence and localization properties are supplied by HF calculations with the same basis set. These results are consistent with the ET spectral features, where the resonance at 0.84 eV can be ascribed to the unresolved contributions of the (close-in-energy) σ^*_{CS} and π^*_{CO} empty MOs and the resonance at 3.1 eV to electron capture into the fourth (σ^*_{CS}) empty MO.

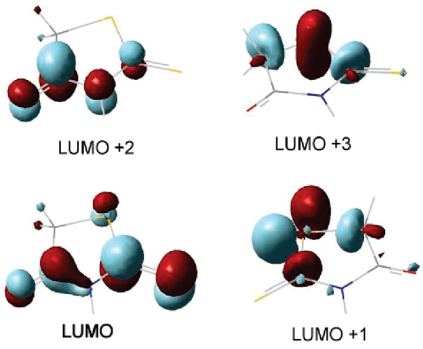

Figure 2. Representation of the four lowest-lying empty MOs of rhodanine, as supplied by B3LYP/6-31G(d) calculations.

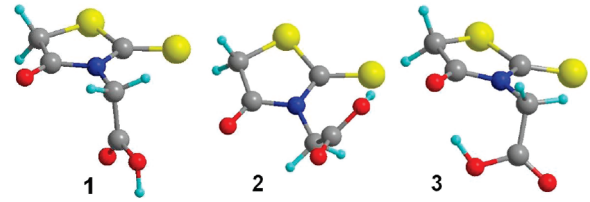

Figure 3. Geometrical structures of the three most stable conformers of rhodanine-3-acetic acid, as supplied by B3LYP/6-31+G(d) calculations.

TABLE 2: Relative Stabilities (eV) of Neutral-State Rhodanine-3-acetic Acid Conformers

conformer	B3LYP/ 6-31G(d)	B3LYP/ 6-31+G(d)	MP2/6-31G(d)// HF/6-31G(d)
1	0.00	0.00	0.00
2	0.232	0.234	0.287
3	0.202	0.219	0.257

Table 1 also reports the VOEs scaled with the two different equations reported above. Although a priori the σ^* scaling employed cannot be considered reliable, the VAEs predicted at 0.8 eV (σ^*_{CS}) and 1.1 eV (π^*_{CO}) are in excellent agreement with the first spectral feature and reproduce the σ^*/π^* energy sequence of the VOEs. The second σ^* VAE is somewhat underestimated. The negative sign of the scaled (π^*_{CS}) LUMO VOE (−0.47 eV) means a positive EA_v.

We note that the calculations predict that not only the LUMO but also the first two filled MOs (close in energy to each other and with a σ lone pair and π character) are mainly localized on the C═S group, in agreement with a photoelectron study of **Rd**[17] and photochemical reactions with metal complexes indicating that rhodanine acts as a monodentate ligand, via the sulfur atom of the C═S double bond.[38]

For the ground neutral state of **Rd-aa**, three local minima, corresponding to different conformations of the substituent (see Figure 3), are calculated at different levels of theory. Their relative energies are reported in Table 2. According to all methods employed, conformers **2** and **3** are at least 0.2 eV less stable than conformer **1** so that their population at 85 °C (sample temperature to obtain DEA spectra) can be evaluated to be <0.15%.

Attempts to record the ET spectrum of **Rd-aa** failed because the maximum temperature (about 105 °C) attainable in the collision chamber of our apparatus is not high enough to obtain a sufficient sample vapor pressure. However, Table 1 reports the calculated VOEs and their scaled values for the most stable conformer **1**. The empty π^* MO (labeled π^*_{COOH} in Table 1) of the substituent is calculated to lie nearly at the same energy as the ring π^*_{CO} MO and very close to the first σ^*_{CS} VAE. Thus, according to the scaled VOEs (see Table 1), the ET spectrum of **Rd-aa** should look quite similar to that of unsubstituted **Rd**. In addition, the energy of the first anion state (EA_v = 0.40 eV) is predicted to be only slightly smaller than that of **Rd**.

EAs can be obtained as the difference between the energy of the lowest anion and that of the ground neutral state, both at the optimized geometry of the neutral species (EA_v) or each with its optimized geometry (EA_a). A proper description of the spatially diffuse electron distributions of anions normally requires a basis set with diffuse functions.[39,40] However, calculated anion state energies decrease as the basis set is expanded so that the choice of a basis set that gives a satisfactory description of the energy and nature of the anion is a priori not

TABLE 3: Total Electronic Energies (eV) of the Vertical and Adiabatic Anion States Relative to the Ground Neutral State

	vertical anion	adiabatic anion
Rd	−0.513	−0.702
Rd-aa		
conformer **1**	−0.517	−0.749
conformer **2**	−0.882	−1.044
conformer **3**	−0.805	−1.051

obvious.[41] In general, the more stable (bound) is the anion state, the smaller is the need to augment the basis set with diffuse functions. Moreover, when basis sets that include diffuse functions are used, one has to ascertain that the singly occupied MO (SOMO) of the anion is not described as a diffuse function with no physical significance with respect to anion formation.[30,31,35,41]

Table 3 reports the B3LYP energies of the first vertical and adiabatic anion states of **Rd** and **Rd-aa** relative to their neutral ground states, obtained using a basis set (6-31+G(d)) with the smallest addition of diffuse functions, (s- and p-type diffuse functions at the nonhydrogen atoms). This method demonstrated to reproduce accurately the (positive) EAs measured in poly-aromatic hydrocarbons.[42] The localization properties of all the SOMOs of the anion states and LUMOs of the neutral states are very similar to those supplied by the 6-31G(d) basis set (which does not include diffuse functions). The EA_v of **Rd** and **Rd-aa** (conformer **1**) are in good agreement (within 0.1 eV) with those supplied by the scaling procedure. For both molecules, the EA_a is calculated to be not much higher (about 0.2 eV) than the EA_v. Table 3 also reports the energies (relative to the ground neutral state of conformer **1**) of the vertical and adiabatic anion states corresponding to conformers **2** and **3** of **Rd-aa**. The optimized geometries of the anion states are found to be similar to those of the corresponding neutral-state conformers, the main difference being the reduction of the O···H distance on going from neutral conformer **3** (1.842 Å) to the corresponding anion state (1.593 Å). However, in contrast with the neutral molecule, the lowest anion states of conformers **2** and **3** are more stable than that of conformer **1**. These results are confirmed by the VOEs (not reported in Table 1) supplied by the 6-31G(d) basis set for the LUMO of the neutral conformers **2** and **3**, their scaled values leading to EA_v values of 0.89 and 0.85 eV, respectively.

Dissociative Electron Attachment. Figure 4 reports the total anion current measured in gas-phase **Rd** at the walls of the collision chamber (0.8 cm from the electron beam) in the 0−4 eV energy range, as a function of the incident electron energy. An intense and sharp peak is displayed at zero energy, followed by a distinct shoulder at about 0.5 eV and a steadily decreasing signal up to 1−1.5 eV. An additional broad and weak peak is observed around 3 eV, that is, in the energy range of the second resonance displayed by the ET spectrum. An evaluation of the total anion current absolute cross section can be obtained from comparison of absolute cross sections reported in the literature with our measurements on the same compounds (see ref 43 for more details). Application of this procedure leads to an absolute cross section with an order of magnitude of 10^{-15} cm^2 for the zero-energy peak. However, due to the relatively low volatility of **Rd** and the fact that, in the apparatus employed, the sample vapor pressure is measured outside the collision chamber, this value has to be considered as an upper limit.

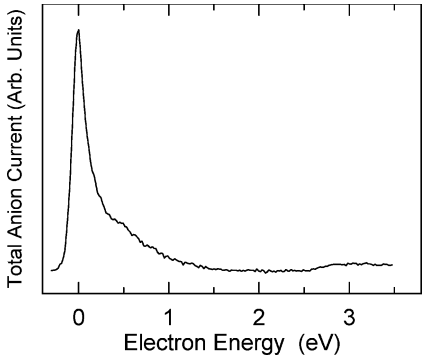

Figure 4. Total anion current, as a function of the incident electron energy, measured in gas-phase rhodanine.

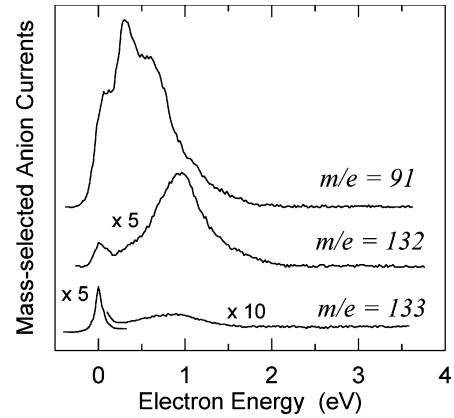

Figure 5. Mass-selected anion currents, as a function of the incident electron energy, measured in gas-phase rhodanine.

TABLE 4: Peak Energies (eV) Measured in the Mass-Selected Negative Currents and Relative Intensities (from Peak Heights)

m/e	anion	peak energy	rel intens
133	M^-	0.00	5.0
		0.9	0.8
132	$(M-H)^-$	0.9	10.0
91	$(M-H_2CCO)^-$	0.0	
		0.3	100
		0.6 sh	

Figure 5 reports the most intense partial anion currents detected through a mass filter. The anion lifetime (about 1 μs) requested to pass the mass filter is about 2 orders of magnitude larger than that requested to reach the walls of the collision chamber in measurements of the total anion current. This could, in part, determine the smaller relative intensity of the zero-energy peaks in the mass-selected spectra, another factor being kinetic energy discrimination in the anion extraction efficiency of the mass spectrometer. The peak energies of the partial anion currents and their relative intensities are given in Table 4.

The most intense signal, which determines the shoulder at about 0.5 eV in the total anion current, comes from the *m/e* = 91 negative fragment, with a peak at 0.3 eV and a pronounced shoulder at 0.6 eV, indicating that both the σ^* and the π^* resonances observed in ETS around 0.8 eV follow a dissociative channel. The shift to lower energy of the peaks in the DEA spectra with respect to the corresponding resonances observed in ETS is well-understood in terms of shorter lifetime and greater distance to the crossing between the anion and neutral potential curves for the anions formed on the high-energy side of the resonance.[44] The *m/e* = 91 anion fragment is assigned to loss of a neutral ketene molecule ($H_2C{=}C{=}O$) from the parent molecular anion (M^-) to give $HNC(S)S^-$. The calculated thermodynamic energy threshold for this process is about 0.4 eV (see Table 5), in satisfactory agreement with the peak

TABLE 5: B3LYP/6-31+G(d) Total Electronic Energies (eV) Relative to the Ground Neutral State of Rhodanine

m/e	anion	eV
133	M^- diss $(H_2)C-S$ bond (**I**)	−0.789
	M^- diss S−C(S) bond (**II**)	0.344
	M^- diss N−C(O) bond (**III**)	0.326
132	$(M-H)^- + H^\bullet$ (from NH)	0.756
	$(M-H)^- + H^\bullet$ (from CH_2)	1.345
91	$HNC(S)S^- + H_2C{=}C{=}O$	0.434
	$HNC(S)S^-$ (cyc) + $H_2C{=}C{=}O$	2.477
	$H_3CSCS^- + NCO^\bullet$	2.991
	$H_2CSCHS^- + NCO^\bullet$	3.241

position. Incidentally, it should be recalled that the reliability of the basis set for evaluating anion state energies can change for different anion species, depending on their stability relative to the corresponding neutral species. A local minimum for formation of the same anion fragment with the structure of a three-membered cycle is also calculated, but its energy is 2 eV higher, as well as the threshold for formation of fragments where the nitrogen atom is replaced by a CH_2 group (see Table 5). In any case, it is noteworthy that production of this negative fragment implies cleavage of two bonds of the ring before the parent molecular anion formed by shape resonance around 0.8 eV decays by re-emission of the extra electron.

Another negative fragment with *m/e* = 132, $(M-H)^-$, gives rise to a rather broad and less intense current peaking at 0.9 eV, thus, likely deriving only from dissociation of the π^*_{CO} resonance. This signal is due to the loss of a hydrogen atom. According to the calculations (see Table 5), the hydrogen atom comes from cleavage of the N−H bond (calculated energy threshold = 0.76 eV), the threshold for dissociation of a C−H bond being predicted to be >1.3 eV.

The *m/e* = 133 anion current, corresponding to M^-, is also detected, with a peak at zero energy and a broader and weaker signal peaking at 0.9 eV (see Figure 5). The signal at zero energy can be associated with formation of vibrationally excited levels of the ground anion state, according to the usual interpretation of long-lived parent anions found at thermal electron energy in a number of compounds. The observation of parent molecular anions at energies above zero is much less common, a few known examples being *p*-benzoquinone,[45] azobenzene,[46,47] anthraquinone,[48] pyromellitic acid imide,[49] and chlorodifluoroacetic acid.[50] In fact, the measured intensity of the *m/e* = 133 current at 0.9 eV is about 8% (see Table 4) relative to that of the $(M-H)^-$ fragment at the same energy, and the two signals have similar shapes. This *m/e* = 133 yield at 0.9 eV is nearly equal, within experimental limits, to that (6%) expected for the contribution from the $(M-H)^-$ fragment due to the isotope abundances of the various elements. We thus assign only the zero-energy peak with *m/e* = 133 to M^-. In the present case, it is also to be noted that breaking of a single ring bond would leave the mass of the dissociated parent anion unchanged so that the M^- current observed at zero energy is not necessarily associated with the parent molecular anion. Table 5 reports the calculated energy thresholds for production of the dissociated molecular anions represented in Figure 6. According to the calculations, dissociation of the $(H_2)C-S$ bond gives a molecular anion (labeled **I** in Figure 6) even more stable than the parent anion, whereas the threshold for cleavage of the S−C(S) or N−C(O) bonds (to give molecular anions **II** and **III**) is predicted to be about 0.3 eV.

Figure 7 reports the total anion current measured in gas-phase **Rd-aa**, as a function of the incident electron energy, in the 0−4 eV energy range. In addition to the sharp and intense zero-energy peak, a shoulder at 0.3 eV and a broader (unresolved) signal at higher energy are observed. Due to the low volatility of **Rd-aa**, not even a rough evaluation of the absolute total cross section based on the pressure measured in the main vacuum chamber is possible. However, comparison of the electron beam attenuations indicates that the total cross section at zero energy of **Rd-aa** is likely even larger than that of **Rd**.

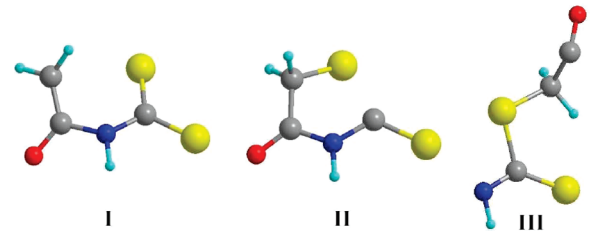

Figure 6. Geometrical structures of dissociated molecular anions of rhodanine, as supplied by B3LYP/6-31+G(d) calculations.

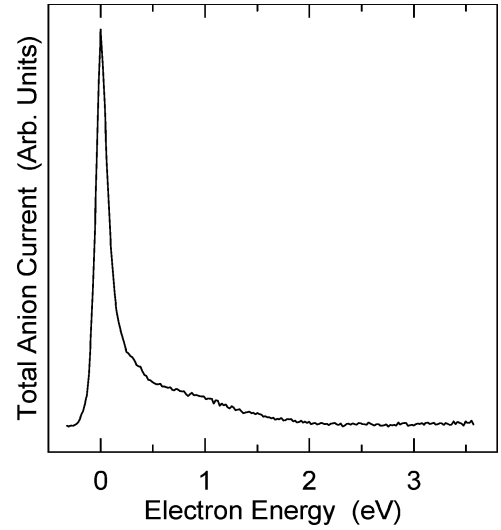

Figure 7. Total anion current, as a function of the incident electron energy, measured in gas-phase rhodanine-3-acetic acid.

Figure 8 displays the most intense partial anion currents detected through a mass filter, with a sample temperature of about 80 °C. The energies of the maxima and their relative yields, as evaluated from the peak heights, are reported in Table 6. By comparison with the DEA spectrum of **Rd**, it is evident, at first glance, that the presence of the CH_2COOH substituent opens a variety of dissociative decay channels of the molecular anion, mainly at thermal electron energies.

The most intense current is observed at zero energy and *m/e* = 147. This negative species corresponds to the loss of a neutral CO_2 molecule from the molecular anion and is plausibly assigned to the *N*-methylrhodanine anion. In agreement, the calculations predict (see Table 7) that these products of dissociation are more stable than the parent molecular anion. The second most abundant negative fragment is found at *m/e* = 75, with a peak at zero energy and a shoulder at 0.3 eV. It should be noted that its intensity relative to *m/e* = 147 (55% at 80 °C) was found to be temperature-dependent, changing from 30% at about 65 °C to 130% at about 95 °C. This finding suggests that the negative species with *m/e* = 147 can, in turn, dissociate to give the smaller *m/e* = 75 anion. On energetic grounds (see Table 7), the latter is assigned to the trigonal (nearly planar, with a central carbon atom) radical anion $C(S)(O)(NH)^{\bullet-}$, formed with the neutral pentacyclic diketone **10** (see Chart 2). This radical anion is calculated to be 0.658

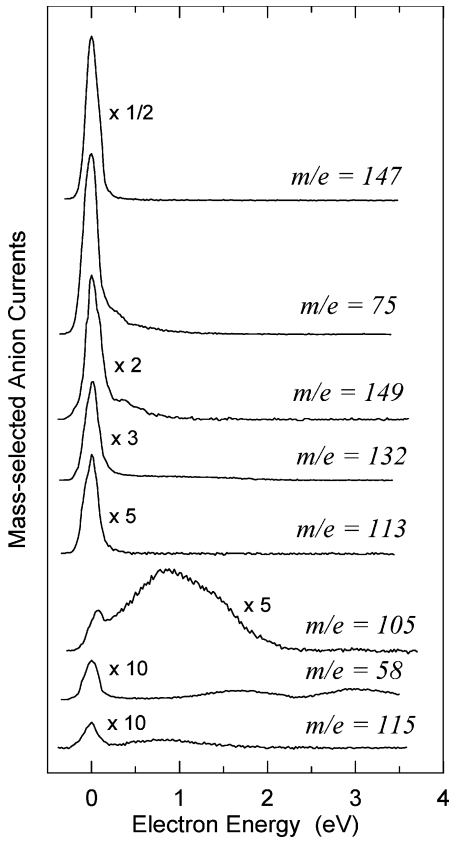

Figure 8. Mass-selected anion currents, as a function of the incident electron energy, measured in gas-phase rhodanine-3-acetic acid.

TABLE 6: Peak Energies (eV) Measured in the Mass-Selected Negative Currents and Relative Intensities (From Peak Heights)

m/e	anion	peak energy	rel intens
190	$(M-H)^-$	0.8	1.0
149	$(M-H_2CCO)^-$	0.00	22
		0.4 sh	
147	$(M-CO_2)^-$	0.00	100
132	$(M-CH_2COOH)^-$	0.02	10
115	$(M-CS_2)^-$	0.0	1.0
		0.9	0.3
113	$(M-CS_2-H_2)^-$	0.00	6
105	$(M-CO_2-H_2CCO)^-$	0.9	5
76	CS_2^-	0.8	≤1
75	$C(S)(O)(NH)^{\bullet -}$	0.00	55
		0.3 sh	5
58	SCN^- or $CH_2CO_2^-$	0.00	1.2
		1.7	0.3
		3.1	0.4

eV more stable than its S=C=N−OH^- linear isomer, probably more expected. Other possible fragmentation products with calculated low (<0.22 eV) thermodynamic thresholds and including a negative species with *m/e* = 75 are listed in Table 7. Anyway, all of these fragmentation pathways are very complex and imply cleavage of several bonds with extensive rearrangements.

The third most intense negative fragment, with *m/e* = 149, is due to loss of a neutral $H_2C=C=O$ molecule from the molecular anion, as observed in rhodanine. This negative current also peaks at zero energy, with a shoulder at about 0.4 eV. Consistently, the calculated energy threshold is very close to zero. Negative currents at zero energy are also observed at *m/e* = 132 and *m/e* = 113, the former corresponding to loss of the

TABLE 7: B3LYP/6-31+G(d) Total Electronic Energies (eV) Relative to the Most Stable Neutral-State Conformer (1) of Rhodanine-3-acetic Acid

m/e	anion	eV
191	M^- diss $(H_2)C-S$ bond (**4a**$^-$)	−0.952
	M^- diss $(H_2)C-S$ bond (**4b**$^-$)	−1.051
	M^- diss $S-C(=S)$ bond (**5a**$^-$)	0.199
	M^- diss $S-C(=S)$ bond (**5b**$^-$)	0.036
190	$(M-H)^-$	0.785
149	$^{\bullet}SC(S)N(H)CH_2COO^- + H_2C=C=O$	0.076
147	*N*-methylrhodanine$^-$ + CO_2	−1.075
132	$(rhodanine-H)^- + CH_3COO^{\bullet}$	−0.224
	$(rhodanine-H)^- + {}^{\bullet}CH_2COOH$	−0.165
115	$^{\bullet}CH_2C(O)N(H)CH_2COO^- + CS_2$	−0.494
	pentacyc **6**$^-$ + CS_2	0.215
	hexacyc **7**$^-$ + CS_2	0.737
113	pentacyc **8**$^-$ + H_2 + CS_2	−0.570
	hexacyc **9**$^-$ + H_2 + CS_2	0.402
105	$^{\bullet}SC(S)N(H)CH_2^- + H_2C=C=O + CO_2$	0.486
	$^{\bullet}SC(S)N(H)CH_2^-$ + 3-*O*-cyclobutan-1,2-dione	1.393
76	CS_2^- + pentacyc **6**	−0.334
75	$C(S)(O)(NH)^{\bullet -}$ + SC(O)$(CH_2)_2$C(O) cyc **10**	−0.118
	$H_3CC(S)O^- + CO_2 + {}^{\bullet}H_2C-N=C=S$	0.070
	$C(S)(O)(NH)^{\bullet -}$ + SC(O)CH_2C(O)CH_2 cyc **11**	0.206
	$H_3CC(S)O^- + O=C=S + {}^{\bullet}H_2C-N=C=O$	0.219
58	$SCN^- + {}^{\bullet}SCH_2C(O)CH_2COOH$	−0.185
	CH_2COO^- + rhodanine	0.313

CHART 2

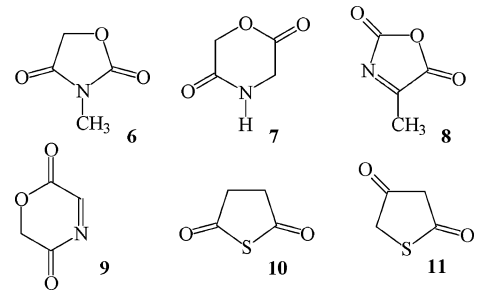

substituent. According to the calculations, the anion (**Rd**−H)$^-$ (*m/e* = 132) and either of the two neutral radicals, $CH_3COO^{\bullet}$ or $^{\bullet}CH_2COOH$, are more stable than neutral **Rd-aa**. The *m/e* = 113 negative fragment is obtained by loss of the neutral molecules CS_2 and H_2. According to the calculations, these two molecules and the pentacyclic anion **8**$^-$ (see Chart 2) can be formed at zero energy, lying lower in energy than neutral **Rd-aa**.

A relatively intense current peaking at 0.9 eV is due to the *m/e* = 105 anion fragment, likely generated by direct loss of the $H_2C=C=O$ and CO_2 neutral molecules from the molecular anion or sequential loss of $H_2C=C=O$ or CO_2, respectively, from the *m/e* = 147 or *m/e* = 149 negative fragments. Consistently, the thermodynamic threshold for formation of these two molecules and the radical anion $^{\bullet}SC(S)N(H)CH_2^-$ from **Rd-aa** is calculated to be 0.49 eV. In principle, 3-*O*-cyclobutan-1,2-dione could be formed, instead, of the two small neutral molecules, but this hypothesis is not supported by the calculated energy threshold (1.4 eV).

Other signals were observed with smaller intensity. The currents with *m/e* = 115 and *m/e* = 76 correspond to the $(M-CS_2)^-$ and CS_2^- negative fragments. Both display weak maxima at zero energy and at 0.8−0.9 eV, although the zero-energy peak of the latter is mostly due to isotopes of the intense *m/e* = 75 anion. The energies of possible negative and neutral fragments are reported in Table 7. A weak signal with *m/e* = 58 displays maxima at 0.0, 1.7, and 3.1 eV. This negative

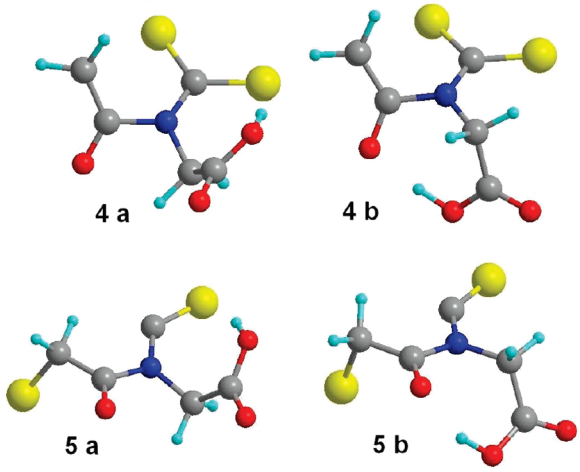

Figure 9. Geometrical structures of dissociated molecular anions of rhodanine-3-acetic acid, as supplied by B3LYP/6-31+G(d) calculations.

fragment could be SCN^- or $CH_2CO_2^-$ (see Table 7). The $(M-H)^-$ fragment with $m/e = 190$, due to cleavage of the carboxylic O−H bond and with a maximum around 0.8 eV (calculated energy threshold = 0.79 eV), was observed, as expected, on the basis of previous DEAS studies of acids[50,51] and alcohols.[52] In the present case, however, its intensity is small (1% relative to the $m/e = 147$ signal at zero energy). Finally, only a very weak signal (about 0.1% relative to $m/e = 147$) at zero energy from the molecular anion ($m/e = 191$) could be observed.

As found for **Rd**, according to calculations, cleavage of the H_2C-S bond of the parent molecular anion leads to molecular anions (**4a** and **4b** in Figure 9) more stable than the parent anion itself (see Table 7), whereas a small (<0.2 eV) energy threshold is predicted for dissociation of the S−C(=S) bond to give molecular anions **5a** and **5b**. However, the almost complete absence of a $m/e = 191$ current and the variety of negative fragments observed at zero energy suggest that the dissociation channels of the parent anion are not limited to cleavage of a single ring bond.

Conclusions

The empty-level electronic structures of rhodanine (**Rd**) and its 3-acetic acid derivative (**Rd-aa**) were investigated by means of electron transmission and dissociative electron attachment (DEA) spectroscopies, with the support of B3LYP calculations, in connection with the possible use of **Rd-aa** as an electron acceptor anchored to TiO_2 in dye-sensitized solar cells. In both compounds, the first anion state, with mainly π^* (C=S) character, is predicted to be stable. Occupation of the first empty σ^* MO, with S−C antibonding character, and of the mainly ring π^* (C=O) MO gives rise to temporary anion states below 1 eV. At about the same energy, **Rd-aa** possesses an additional anion state, associated with electron capture into the mainly π^* (C=O) MO of the carboxyl substituent.

Measurements of the total anion current, as a function of the incident electron energy, show that, in both compounds, the cross section has a sharp and intense maximum at zero energy, followed by a weaker signal in the 0.3−1.5 eV range. The mass-selected DEA spectra show that, in **Rd**, the most abundant negative fragments correspond to loss of a ketene ($H_2C=C=O$) molecule or a hydrogen atom from the molecular anion. The former complex dissociation process leads to irreversible decomposition of the pentacyclic ring. Formation of long-lived (≥ 1 μs) molecular anions is also detected at zero energy. This signal ($m/e = 133$) can be due to either the parent molecular anion or a molecular anion generated by cleavage of the ring H_2C-S bond. According to the B3LYP/6-31+G(d) calculations, in fact, this dissociated molecular anion (of both **Rd** and **Rd-aa**) is more stable than the parent anion.

The DEA spectra of **Rd-aa**, in addition to the anion fragments deriving from loss of a neutral ketene molecule or a hydrogen atom, display a great variety of other negative species, mainly produced by capture of thermal electrons. The most intense current, observed at $m/e = 147$, corresponds to loss of a CO_2 molecule from the substituent. Several other negative fragments are generated from complex pathways that include multiple bond ring dissociation and extensive nuclear rearrangements, as in the case of the second most abundant current ($m/e = 75$) ascribed on energetic grounds to the $C(S)(O)(NH)^{\bullet -}$ radical anion. In line with the presence of a great number of dissociative decay channels, only a very weak molecular anion current was detected at zero energy.

Rd-aa bonded to a triphenylamine-based donor moiety through a butadiene bridge was found[9] to possess the electronic requirements for an efficient sensitizer in TiO_2 solar cells, with an encouraging overall conversion efficiency of 5.84%. However, the present DEAS results unfortunately indicate that such a material can hardly achieve the requirement of long-term stability under conditions of excess negative charge. The DEA technique thus emerges as a useful probe for a preventive determination of the stabilities of prospective dye-sensitized solar cell components.

Acknowledgment. A.M. thanks the Italian Ministero dell'Istruzione, dell'Università e della Ricerca, for financial support.

References and Notes

(1) Aberle, A. G. *Thin Solid Films* **2009**, *517*, 4706.
(2) Krebs, F. C. *Sol. Energy Mater. Sol. Cells* **2009**, *93*, 394.
(3) Grätzel, M. *Nature* **2001**, *414*, 338.
(4) Kamat, P. V.; Schatz, G. C. *J. Phys. Chem. C* **2009**, *113*, 15473.
(5) Robertson, N. *Angew. Chem., Int. Ed.* **2006**, *45*, 2338.
(6) Hamann, T. W.; Jensen, R. A.; Martinson, A. B. F.; Van Ryswyk, H.; Hupp, J. T. *Energy Environ. Sci.* **2008**, *1*, 66.
(7) Segura, J. L.; Martín, N.; Guldi, D. M. *Chem. Soc. Rev.* **2005**, *34*, 31.
(8) Roquet, S.; Cravino, A.; Leriche, P.; Aléveque, O.; Frère, P.; Roncali, J. *J. Am. Chem. Soc.* **2006**, *128*, 3459.
(9) Liang, M.; Xu, W.; Cai, F.; Chen, P.; Peng, B.; Chen, J.; Li, Z. *J. Phys. Chem. C* **2007**, *111*, 4465.
(10) Xu, W.; Peng, B.; Chen, J.; Liang, M.; Cai, F. *J. Phys. Chem. C* **2008**, *112*, 874.
(11) Cutshall, N. S.; Day, C. O.; Prezhdo, M. *Bioorg. Med. Chem. Lett.* **2001**, *11*, 91.
(12) Peet, N. P. *IDrugs* **2000**, *3*, 131.
(13) Sakagami, Y.; Kumeda, Y.; Shibata, M. *Biosci., Biotechnol., Biochem.* **1998**, *62*, 1025.
(14) Gorishniy, V. Y.; Lesyk, R. B. *Farm. Zh. (Kiev, Ukr.)* **1994**, *2*, 52.
(15) Clark, D. A.; Goldstein, S. W.; Hulin, B. U.S. Patent 5,036,079; *Chem. Abstr.* **1992**, *116*, 83663.
(16) Fabretti, A. C.; Franchini, G.; Peyronel, G.; Ferrari, M. *Polyhedron* **1982**, *1*, 633.
(17) Andreocci, M. V.; Cauletti, C.; Sestili, L. *Spectrochim. Acta* **1984**, *40A*, 1087.
(18) Sanche, L.; Schulz, G. J. *Phys. Rev. A* **1972**, *5*, 1672.
(19) Schulz, G. J. *Rev. Mod. Phys.* **1973**, *45*, 378, 423.
(20) Illenberger, E.; Momigny, J. *Gaseous Molecular Ions. An Introduction to Elementary Processes Induced by Ionization*; Steinkopff Verlag: Darmstadt, Germany, 1992.
(21) Modelli, A.; Jones, D.; Rossini, S.; Distefano, G. *Tetrahedron* **1984**, *40*, 3257.
(22) Modelli, A. *Trends Chem. Phys.* **1997**, *6*, 57.

(23) Modelli, A.; Jones, D.; Distefano, G.; Tronc, M. *Chem. Phys. Lett.* **1991**, *181*, 361.
(24) Modelli, A.; Venuti, M.; Szepes, L. *J. Am. Chem. Soc.* **2002**, *124*, 8498.
(25) Modelli, A.; Jones, D.; Distefano, G. *Chem. Phys. Lett.* **1982**, *86*, 434.
(26) Johnston, A. R.; Burrow, P. D. *J. Electron Spectrosc. Relat. Phenom.* **1982**, *25*, 119.
(27) Modelli, A.; Foffani, A.; Scagnolari, F.; Jones, D. *Chem. Phys. Lett.* **1989**, *163*, 269.
(28) Frisch, M. J.; Trucks, G. W.; Schlegel, H. B.; Scuseria, G. E.; Robb, M. A.; Cheeseman, J. R.; Montgomery, J. A.; Vreven, T.; Kudin, K. N.; Burant, J. C.; Millam, J. M.; Iyengar, S. S.; Tomasi, J.; Barone, V.; Mennucci, B.; Cossi, M.; Scalmani, G.; Rega, N.; Petersson, G. A.; Nakatsuji, H.; Hada, M.; Ehara, M.; Toyota, K.; Fukuda, R.; Hasegawa, J.; Ishida, M.; Nakajima, T.; Honda, Y.; Kitao, O.; Nakai, H.; Klene, M.; Li, X.; Knox, J. E.; Hratchian, H. P.; Cross, J. B.; Bakken, V.; Adamo, C.; Jaramillo, J.; Gomperts, R.; Stratmann, R. E.; Yazyev, O.; Austin, A. J.; Cammi, R.; Pomelli, C.; Ochterski, J. W.; Ayala, P. Y.; Morokuma, K.; Voth, G. A.; Salvador, P.; Dannenberg, J. J.; Zakrzewski, V. G.; Dapprich, S.; Daniels, A. D.; Strain, M. C.; Farkas, O.; Malick, D. K.; Rabuck, A. D.; Raghavachari, K.; Foresman, J. B.; Ortiz, J. V.; Cui, Q.; Baboul, A. G.; Clifford, S.; Cioslowski, J.; Stefanov, B. B.; Liu, G.; Liashenko, A.; Piskorz, P.; Komaroni, I.; Martin, R. L.; Fox, D. J.; Keith, T.; Al-Laham, M. A.; Peng, C. Y.; Nanayakkara, A.; Challacombe, M.; Gill, P. M. W.; Johnson, B.; Chen, W.; Wong, M. W.; Gonzalez, C.; Pople, J. A. *Gaussian 03*, revision D.01; Gaussian Inc.: Wallingford, CT, 2004.
(29) Becke, A. D. *J. Chem. Phys.* **1993**, *98*, 5648.
(30) Staley, S. S.; Strnad, J. T. *J. Phys. Chem.* **1994**, *98*, 161.
(31) Guerra, M. *Chem. Phys. Lett.* **1990**, *167*, 315.
(32) Chen, D. A.; Gallup, G. A. *J. Chem. Phys.* **1990**, *93*, 8893.
(33) Simons, J.; Jordan, K. D. *Chem. Rev.* **1987**, *87*, 535.
(34) Lane, N. F. *Rev. Mod. Phys.* **1980**, *52*, 29.
(35) Modelli, A. *Phys. Chem. Chem. Phys.* **2003**, *5*, 2923.
(36) Modelli, A.; Szepes, L. *Chem. Phys.* **2003**, *286*, 165.
(37) Pshenichnyuk, S. A.; Asfandiarov, N. L.; Burrow, P. D. *Russ. Chem. Bull., Int. Edit.* **2007**, *56*, 1268.
(38) Subasi, E.; Ercag, A.; Sert, S.; Senturk, O. S. *Synth. React. Inorg., Met.-Org., Nano-Met. Chem.* **2006**, *36*, 705.
(39) Hehre, W. J.; Radom, L.; Schleyer, P. v. R.; Pople, J. A. *Ab initio Molecular Orbital Theory*; Wiley: New York, 1986.
(40) Dunning, T. H., Jr.; Peterson, K. A.; Woon, D. E. *Basis Sets: Correlation Consistent Sets in the Encyclopedia of Computational Chemistry*; Schleyer, P. v. R., Ed.; John Wiley: Chichester, U.K., 1998.
(41) Modelli, A.; Hajgató, B.; Nixon, F. J.; Nyulászi, L. *J. Phys. Chem. A* **2004**, *108*, 7440.
(42) Modelli, A.; Mussoni, L.; Fabbri, D. *J. Phys. Chem. A* **2006**, *110*, 6482.
(43) Modelli, A. *J. Phys. Chem. A* **2005**, *109*, 6193.
(44) O'Malley, T. F. *Phys. Rev.* **1966**, *150*, 14.
(45) Allan, M. *Chem. Phys.* **1983**, *81*, 235.
(46) Vasil'ev, Y. V.; Mazunov, V. A.; Nazirov, E. R. *Org. Mass Spectrom.* **1991**, *26*, 739.
(47) Modelli, A.; Burrow, P. D. *Phys. Chem. Chem. Phys.* **2009**, *11*, 8448.
(48) Asfandiarov, N. L.; Fokin, A. I.; Lukin, V. G.; Nafikova, E. P.; Lomakin, G. S.; Fal'ko, V. S.; Chizhov, Yu. V. *Rapid Commun. Mass Spectrom.* **1999**, *13*, 1116.
(49) Khvostenko, O. G.; Tuimedov, G. M. *Rapid Commun. Mass Spectrom.* **2006**, *20*, 3699.
(50) Kopyra, J.; König-Lehmann, C.; Szamrej, I.; Illenberger, E. *Int. J. Mass Spectrom.* **2009**, *285*, 131.
(51) Asfandiarov, N. L.; Pshenichnyuk, S. A.; Fokin, A. I.; Lukin, V. G.; Fal'ko, V. S. *Rapid Commun. Mass Spectrom.* **2002**, *16*, 1760.
(52) Ibanescu, B. C.; May, O.; Monney, A.; Allan, M. *Phys. Chem. Chem. Phys.* **2007**, *9*, 3163.

JP910595V